INTERNATIONAL JOURNAL FOR NUMERICAL METHODS IN FLUIDS, VOL. 9, 1221–1234 (1989)

THE SIMPLE LAYER POTENTIAL METHOD OF FUNDAMENTAL SOLUTIONS FOR CERTAIN BIHARMONIC PROBLEMS

ANDREAS KARAGEORGHIS

Department of Mathematics, University College of Wales, Aberystwyth SY23 3BZ, U.K.

AND

GRAEME FAIRWEATHER

Departments of Mathematics and Engineering Mechanics, University of Kentucky, Lexington, KY 40506, U.S.A.

SUMMARY

A novel formulation of the method of fundamental solutions for the numerical solution of plane biharmonic problems, based on the simple layer potential representation of Fichera, is presented. The applicability and accuracy of the method are demonstrated by examining its performance on a set of practical problems arising in Stokes fluid flow.

KEY WORDS Biharmonic equation Stokes flow Simple layer potential Method of fundamental solutions

1. INTRODUCTION

In recent studies by Karageorghis and Fairweather,[1,2] two formulations of the method of fundamental solutions have been used successfully for the numerical solution of a variety of biharmonic problems. Each of these formulations was proposed by Fairweather and Johnston.[3] In this paper we examine a third approach suggested by these authors, which is based on a simple layer potential representation of a biharmonic function given by Fichera.[4]

The biharmonic problem considered in this paper is

$$\nabla^2(\nabla^2\psi(p)) \equiv \nabla^4\psi(p) = 0, \quad p \in \Omega, \tag{1}$$

subject to

$$B_1\psi(p) \equiv \alpha(p) + \frac{\partial\psi}{\partial x_p}(p) = 0,$$

$$B_2\psi(p) \equiv \beta(p) + \frac{\partial\psi}{\partial y_p}(p) = 0, \quad p \in \partial\Omega, \tag{2}$$

where Ω is a bounded domain in the plane with boundary $\partial\Omega$, ∇^2 denotes the Laplacian, $\partial/\partial x_p$ and $\partial/\partial y_p$ denote the partial derivatives with respect to x_p and y_p respectively, and α and β are prescribed functions of position. Problems of this type arise, for example, in fluid flow problems, where ψ denotes the stream function, and do not have unique solutions—clearly $\psi + c$ is a solution of (1), (2), where c is an arbitrary constant. The quantities of interest in such problems are usually

0271-2091/89/101219-14$07.00 *Received July 1988*

derivatives of the solution, in which case this non-uniqueness is inconsequential.

Fichera's simple layer potential representation of a solution ψ of (1), (2) takes the form

$$\psi(p)=\int_{\partial\Omega}\left\{\sigma(q)\frac{\partial}{\partial x_q}G(p,q)+\mu(q)\frac{\partial}{\partial y_q}G(p,q)\right\}\mathrm{d}s_q,\quad p\in\bar{\Omega},\tag{3}$$

where σ and μ are density functions defined on $\partial\Omega$ and are determined so that ψ satisfies the prescribed boundary conditions on $\partial\Omega$. The function $G(p, q)$ is a fundamental solution of the biharmonic equation, namely

$$G(p,q)=-\tfrac{1}{4}r^2(p,q)\log r^2(p,q),$$

where $r(p, q)$ is the distance between the points $p=(x_p, y_p)$ and $q=(x_q, y_q)$. Since

$$\frac{\partial G(p,q)}{\partial x_q}=\tfrac{1}{2}(x_p-x_q)[\log r^2(p,q)+1]\quad\text{and}\quad\frac{\partial G(p,q)}{\partial y_q}=\tfrac{1}{2}(y_p-y_q)[\log r^2(p,q)+1],$$

equation (3) becomes

$$\psi(p)=\tfrac{1}{2}\int_{\partial\Omega}[\sigma(q)(x_p-x_q)+\mu(q)(y_p-y_q)]K(p,q)\,\mathrm{d}s_q,\quad p\in\bar{\Omega},\tag{4}$$

where

$$K(p,q)=\log r^2(p,q)+1,$$

a fundamental solution of Laplace's equation. Based on (4), boundary integral formulations of biharmonic problems of the form (1), (2) have been examined by Black *et al.*,[5] Hsiao and MacCamy[6] and Richter.[7]

In the present formulation of the method of fundamental solutions, we define an approximation ψ_N to ψ by

$$\psi_N(\mathbf{c},\mathbf{d},\mathbf{t},p_i)=\sum_{j=1}^{N}[c_j(x_{p_i}-x_{t_j})+d_j(y_{p_i}-y_{t_j})]K(p_i,t_j),\tag{5}$$

where

$$\mathbf{c}=[c_1,c_2,\ldots,c_N],\qquad\mathbf{d}=[d_1,d_2,\ldots,d_N],\qquad\mathbf{t}=[x_{t_1},y_{t_1},x_{t_2},y_{t_2},x_{t_3},y_{t_3},\ldots,x_{t_N},y_{t_N}],$$

(x_{p_i}, y_{p_i}) are the co-ordinates of the point p_i, with $p_i\in\bar{\Omega}$, and (x_{t_j}, y_{t_j}) are the co-ordinates of the singularity t_j, a point outside $\bar{\Omega}$. This representation of a biharmonic function is motivated by considering Fichera's representation (4) with respect to an 'auxiliary boundary' $\partial\Omega_a$; enclosing the region Ω, and replacing the integral by some quadrature formula with nodes t_j, $j=1,\ldots,N$; c.f. Oliveira.[8] The goal is to determine the locations of these points (and in essence the auxiliary boundary $\partial\Omega_a$) and the values of the coefficients c_j and d_j so that the function ψ_N satisfies the boundary conditions (2) in some sense. As in previous formulations of the method of fundamental solutions,[1, 2] this is done by a least squares fit of ψ_N to the boundary data; that is, by choosing points p_i, $i=1,\ldots,M$, on $\partial\Omega$ and minimizing the functional

$$F(\mathbf{c},\mathbf{d},\mathbf{t})=\sum_{i=1}^{M}\{|B_1\psi_N(\mathbf{c},\mathbf{d},\mathbf{t},p_i)|^2+|B_2\psi_N(\mathbf{c},\mathbf{d},\mathbf{t},p_i)|^2\},\tag{6}$$

which is linear in the coefficients $c_j, d_j, j=1,\ldots,N$, but non-linear in the t_j's. The minimization is performed using a non-linear least squares algorithm, with the number of boundary points taken to be approximately three times the number of unknowns, i.e. $M\approx 12N$, as recommended by Ho-Tai *et al.*[9]

2. SOLUTION OF THE MINIMIZATION PROBLEM

The non-linear least squares problem is solved via the routine LMDIF (from MINPACK), which is based on a modified version of the Levenberg–Marquardt algorithm. The subroutine LMDIF minimizes

$$F=\sum_{i=1}^{2M}|f_i|^2,$$

where

$$f_i=\alpha(p_i)+\frac{\partial\psi_N(p_i)}{\partial x_p},\quad i=1,2,\ldots,M, \tag{7}$$

and

$$f_i=\beta(p_i)+\frac{\partial\psi_N(p_i)}{\partial y_p},\quad i=M+1,\ldots,2M. \tag{8}$$

The routine LMDIF requires the user to provide starting values for all the variables. In general the boundary points are placed uniformly around the boundary and initially the singularities are placed uniformly outside the region at a fixed distance from the boundary points, as described by Karageorghis and Fairweather.[1] Initially all of the coefficients c_j and d_j are set equal to unity. The computational effort involved in the use of LMDIF is measured in terms of the number of function evaluations, FEV; that is, the number of times the vector $\mathbf{f}=[f_1,f_2,\ldots,f_{2M}]$ is evaluated. The minimization process terminates when either convergence to a user-specified tolerance is achieved or the user-specified limit on the number of function evaluations is reached.

In implementing the present MFS, advantage may be taken of certain symmetries the boundary value problem in question may possess, for example, symmetry about one co-ordinate axis. Expressions for (7) and (8) in this case are given in the Appendix.

The implementation also includes a technique introduced by MacDonell,[10] which has been used effectively in previous MFS formulations to improve the convergence rate of the minimization process. The idea is to begin the process with $N1$ singularities and M1 boundary points and to perform FEV1, say, function evaluations. The number of singularities is then increased to $N2$ and the number of boundary points to $M2$, where $M2=M1+12(N2-N1)$. A number, FEV2, of function evaluations is then performed, after which the number of singularities can be increased to $N3$ with a corresponding increase in the number of boundary points to $M3$, with $M3=M2+12(N3-N2)$. In subsequent examples this technique is referred to as the improved version of the MFS.

It should be noted that the subroutine LMDIF does not require the user to provide the Jacobian but calculates an approximation to it. The use of LMDER, also from MINPACK, might improve the efficiency of the minimization process but would increase significantly the complexity of the code since this routine requires the user to supply the exact Jacobian. In neither of these codes can one exploit the structure of the functional (6) in which the coefficients c_j, d_j, $j=1,\ldots,N$, are linear and only the co-ordinates of the singularities appear non-linearly.

3. NUMERICAL EXAMPLES

In this section the method is tested on three problems arising in Stokes fluid flow. All of the computations were performed in double precision on an IBM 3090/300E computer at the University of Kentucky.

3.1. *Example 1—Fully developed Poiseuille flow*

In this simple example we examine fully developed Poiseuille flow in a unit square. This problem was solved by Black *et al.*[5] using a boundary element method based on Fichera's simple layer potential representation (4).

The streamfunction ψ satisfies the biharmonic equation (1) subject to the boundary conditions shown in Figure 1. The solution of this problem is

$$\psi(x, y)=\tfrac{3}{2}(y-\tfrac{4}{3}y^3).$$

This problem possesses symmetry about the y-axis, which is exploited in the implementation of the MFS. Numerical experiments were carried out for various values of M, N and FEV. In Table I the magnitude of the error in the velocity $\partial\psi/\partial y$ is presented on a $0{\cdot}1 \times 0{\cdot}2$ grid on the region $[-\frac{1}{2}, 0]\times[-\frac{1}{2}, \frac{1}{2}]$. (In the table the entries in each cell refer to the top left-hand grid point of the cell.) For each set of parameters it can be seen that the error is uniform throughout this region. Moreover, the efficiency of the improved version of the MFS can also be observed. With fewer degrees of freedom and function evaluations, this method produces more accurate approximations than the basic method. From results (d) and (e) it can be seen that, in this example, little is gained by increasing the number of boundary points. On the other hand, experiments show that an increase in the number of singularities degrades the rate of convergence.

In Table II we tabulate the vorticity $\nabla^2\psi$ on the same grid. In this case there is an indication that the error achieves its maximum on the boundary and, in particular, at the corners of the region.

3.2. *Example 2—The driven cavity problem*

The second example investigated in this study is the driven cavity problem, which describes steady viscous flow in a square cavity with a sliding wall. In recent years, boundary methods for the solution of this problem have been examined by Burgess and Mahajerin,[11] Ingber and

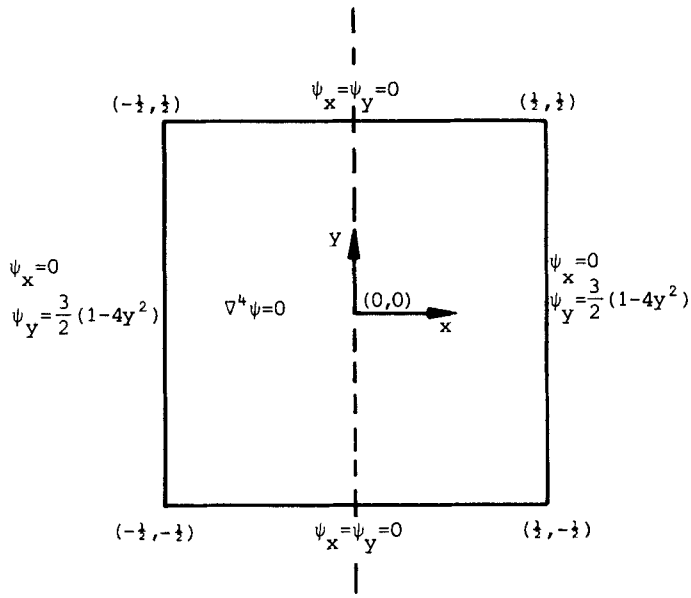

Figure 1. Fully developed Poiseuille flow

Table I. Error in $\partial\psi/\partial y$ for Example 1

(a)	0·2691 (−2)	0·7871 (−3)	0·2272 (−2)	0·2203 (−2)	0·1535 (−2)	0·2321 (−2)
	0·5949 (−3)	0·3704 (−3)	0·2989 (−3)	0·1623 (−3)	0·1147 (−3)	0·2289 (−3)
	0·1484 (−4)	0·1158 (−3)	0·2828 (−4)	0·9001 (−4)	0·5017 (−4)	0·2114 (−4)
	0·5884 (−5)	0·1397 (−4)	0·2891 (−4)	0·2955 (−4)	0·1618 (−4)	0·4403 (−4)
	0·7246 (−4)	0·1567 (−4)	0·4241 (−5)	0·1033 (−4)	0·1807 (−5)	0·1256 (−4)
(b)	0·3412 (−2)	0·3374 (−2)	0·3445 (−2)	0·3422 (−2)	0·3466 (−2)	0·3519 (−2)
	0·2093 (−3)	0·1567 (−3)	0·1994 (−3)	0·1914 (−3)	0·2164 (−3)	0·2434 (−3)
	0·3581 (−4)	0·1967 (−4)	0·3735 (−4)	0·2552 (−4)	0·3598 (−4)	0·4962 (−4)
	0·9358 (−5)	0·1599 (−5)	0·1379 (−4)	0·1097 (−4)	0·3849 (−5)	0·7541 (−6)
	0·4412 (−5)	0·7304 (−6)	0·1032 (−5)	0·1079 (−8)	0·3016 (−5)	0·4696 (−5)
(c)	0·3762 (−2)	0·4089 (−2)	0·4127 (−2)	0·4154 (−2)	0·4182 (−2)	0·4195 (−2)
	0·3731 (−5)	0·1635 (−3)	0·2084 (−3)	0·2374 (−3)	0·2579 (−3)	0·2661 (−3)
	0·2413 (−4)	0·3556 (−4)	0·3622 (−4)	0·3783 (−4)	0·4139 (−4)	0·4346 (−4)
	0·4208 (−5)	0·2197 (−6)	0·3428 (−5)	0·5059 (−5)	0·4355 (−5)	0·3690 (−5)
	0·6292 (−5)	0·2431 (−5)	0·6579 (−6)	0·2732 (−5)	0·3957 (−5)	0·4382 (−5)
(d)	0·4210 (−2)	0·4105 (−2)	0·4057 (−2)	0·4084 (−2)	0·4127 (−2)	0·4146 (−2)
	0·2441 (−3)	0·2715 (−3)	0·2542 (−3)	0·2561 (−3)	0·2658 (−3)	0·2712 (−3)
	0·1324 (−4)	0·2479 (−4)	0·3226 (−4)	0·3654 (−4)	0·4059 (−4)	0·4262 (−4)
	0·9405 (−5)	0·1104 (−4)	0·7703 (−5)	0·5201 (−5)	0·3606 (−5)	0·3015 (−5)
	0·1490 (−4)	0·1476 (−4)	0·1133 (−4)	0·8745 (−5)	0·6700 (−5)	0·5855 (−5)
(e)	0·3187 (−2)	0·2895 (−2)	0·3070 (−2)	0·3142 (−2)	0·3246 (−2)	0·3314 (−2)
	0·2355 (−3)	0·1163 (−3)	0·1879 (−3)	0·1958 (−3)	0·2238 (−3)	0·2500 (−3)
	0·5930 (−4)	0·3518 (−4)	0·4073 (−4)	0·2882 (−4)	0·3711 (−4)	0·4855 (−4)
	0·1849 (−4)	0·8024 (−5)	0·2174 (−5)	0·1917 (−6)	0·3564 (−6)	0·6358 (−6)
	0·1377 (−7)	0·1738 (−5)	0·8014 (−5)	0·7927 (−5)	0·4012 (−5)	0·2157 (−5)
	0·9340 (−3)	0·6037 (−4)	0·1141 (−2)	0·1662 (−2)	0·1015 (−2)	0·1533 (−2)
	0·4419 (−3)	0·2802 (−3)	0·2686 (−3)	0·2308 (−3)	0·4822 (−4)	0·2458 (−3)
	0·8249 (−4)	0·6249 (−4)	0·1587 (−4)	0·9369 (−4)	0·2926 (−4)	0·2682 (−4)
	0·4244 (−4)	0·1869 (−4)	0·4852 (−5)	0·1370 (−4)	0·5430 (−5)	0·1860 (−4)
	0·1230 (−5)	0·1834 (−4)	0·1817 (−4)	0·2052 (−4)	0·1336 (−4)	0·3393 (−4)

(a) $M=80$, $N=8$, FEV = 350.
(b) $M=80$, $N=8$, FEV = 650.
(c) $M=100$, $N=10$, FEV = 1000.
(d) $M1=44$, $N1=5$, FEV1 = 200, $M2=68$, $N2=7$, FEV2 = 500.
(e) $M1=60$, $N1=5$, FEV1 = 200, $M2=84$, $N2=7$, FEV2 = 500.

Mitra,[12] Karageorghis and Fairweather[1,2] and Kelmanson.[13] The flow region and boundary conditions for this problem are shown in Figure 2.

The problem is symmetric about the y-axis and this is exploited in the present formulation of the MFS. Complicating this problem are the boundary singularities at the corners $(-\frac{1}{2}, \frac{1}{2})$ and $(\frac{1}{2}, \frac{1}{2})$. As in Karageorghis and Fairweather,[1,2] in a neighbourhood of a corner singularity a denser grid is imposed by choosing boundary points at a distance

$$d_j = 0{\cdot}5\,[j/M_1]^{\rho}$$

from the corner. The subscript j refers to the jth boundary point from the singularity, M_1 is the number of boundary points on the halves of the sides adjacent to the corner near the singularity,

Table II. Error in $\nabla^2\psi$ for Example 1

(a)	0.4884 (−1)	0·2575 (−1)	0·1058 (−2)	0·5138 (−2)	0·1562 (−2)	0·9560 (−2)
	0·3026 (−1)	0·1546 (−1)	0·5545 (−3)	0·3150 (−2)	0·1185 (−2)	0·5743 (−2)
	0·4416 (−2)	0·7088 (−2)	0·5314 (−3)	0·3123 (−2)	0·6360 (−4)	0·3421 (−2)
	0·2329 (−2)	0·2962 (−2)	0·3124 (−2)	0·1109 (−2)	0·8764 (−3)	0·1654 (−2)
	0·2359 (−2)	0·1596 (−3)	0·1916 (−3)	0·6574 (−4)	0·1042 (−3)	0·1735 (−3)
(b)	0·1946 (−1)	0·3741 (−2)	0·6579 (−3)	0·1303 (−3)	0·7693 (−3)	0·1167 (−2)
	0·1204 (−1)	0·2878 (−2)	0·3602 (−3)	0·1299 (−3)	0·5275 (−3)	0·7705 (−3)
	0·1141 (−2)	0·8046 (−4)	0·4408 (−4)	0·6358 (−4)	0·7378 (−4)	0·2129 (−3)
	0·1713 (−2)	0·4198 (−3)	0·1976 (−3)	0·2069 (−3)	0·1353 (−4)	0·1290 (−3)
	0·8427 (−3)	0·2018 (−3)	0·5795 (−4)	0·1300 (−4)	0·1689 (−4)	0·2905 (−4)
(c)	0·1454 (−1)	0·3365 (−2)	0·8905 (−3)	0·3308 (−3)	0·2645 (−3)	0·2743 (−3)
	0·9193 (−2)	0·2339 (−2)	0·6316 (−3)	0·2620 (−3)	0·2125 (−3)	0·2164 (−3)
	0·1612 (−2)	0·2954 (−3)	0·6507 (−4)	0·1055 (−4)	0·1488 (−4)	0·2549 (−4)
	0·1048 (−2)	0·3206 (−3)	0·1123 (−3)	0·6034 (−4)	0·3340 (−4)	0·2187 (−4)
	0·6597 (−3)	0·1903 (−3)	0·5764 (−4)	0·2235 (−4)	0·1487 (−4)	0·1413 (−4)
(d)	0·1375 (−1)	0·3568 (−2)	0·8610 (−3)	0·3196 (−3)	0·2384 (−3)	0·2399 (−3)
	0·8375 (−2)	0·2089 (−2)	0·5280 (−3)	0·1768 (−3)	0·1173 (−3)	0·1153 (−3)
	0·1063 (−2)	0·2424 (−3)	0·5202 (−4)	0·1024 (−4)	0·5857 (−5)	0·1262 (−4)
	0·1888 (−2)	0·4305 (−3)	0·1102 (−3)	0·2255 (−4)	0·1540 (−4)	0·2895 (−4)
	0·3917 (−3)	0·9020 (−4)	0·2202 (−4)	0·4851 (−5)	0·4575 (−5)	0·8593 (−5)
(e)	0·1533 (−1)	0·4733 (−2)	0·3800 (−3)	0·1587 (−3)	0·6791 (−3)	0·1041 (−2)
	0·9057 (−2)	0·2192 (−2)	0·2149 (−3)	0·8490 (−4)	0·3866 (−3)	0·6000 (−3)
	0·1315 (−2)	0·1629 (−3)	0·4905 (−4)	0·6197 (−4)	0·4164 (−4)	0·1556 (−3)
	0·1868 (−2)	0·3874 (−3)	0·1748 (−4)	0·8335 (−4)	0·7711 (−4)	0·1833 (−3)
	0·2668 (−3)	0·5879 (−4)	0·6345 (−4)	0·5123 (−4)	0·1739 (−4)	0·5245 (−4)
	0·3232 (−1)	0·2501 (−1)	0·1301 (−2)	0·5548 (−2)	0·1159 (−2)	0·9040 (−2)
	0·1945 (−1)	0·1524 (−1)	0·8655 (−3)	0·3483 (−2)	0·7332 (−3)	0·5311 (−2)
	0·8072 (−2)	0·5136 (−2)	0·6557 (−3)	0·2667 (−2)	0·6531 (−4)	0·2876 (−2)
	0·3319 (−2)	0·2496 (−2)	0·1658 (−2)	0·1699 (−2)	0·7186 (−3)	0·1901 (−2)
	0·1265 (−2)	0·6017 (−3)	0·8401 (−3)	0·3163 (−3)	0·2732 (−3)	0·5142 (−3)

(a) $M=80$, $N=8$, FEV = 550.
(b) $M=80$, $N=8$, FEV = 750.
(c) $M=100$, $N=10$, FEV = 1200.
(d) $M1=60$, $N1=5$, FEV1 = 300, $M2=92$, $N2=8$, FEV2 = 600.
(e) $M1=60$, $N1=5$, FEV1 = 200, $M2=84$, $N2=7$, FEV2 = 800.

and ρ is a parameter controlling the degree of density. If $\rho=1$, a uniform distribution results, and if $\rho>1$, a refined distribution is obtained in the neighbourhood of the singularity. The value $\rho=2$ was used in all of the experimental work.

One of the quantities of interest in this problem is the velocity $\partial\psi/\partial y$ along the centreline of the flow, the line $x=0$ in Figure 2. The velocity profile along this line is presented in Figure 3 for $M1=100$, $N1=10$, FEV1 = 1000, $M2=136$, $N2=13$ and FEV2 = 3500. The stagnation point was found to be a distance 0·76 from the furthest clamped edge, in contrast to 0·71 predicted by Burgess and Mahajerin.[11] The location of the stagnation point obtained by the MFS agrees exactly with the value obtained by Kelmanson.[13]

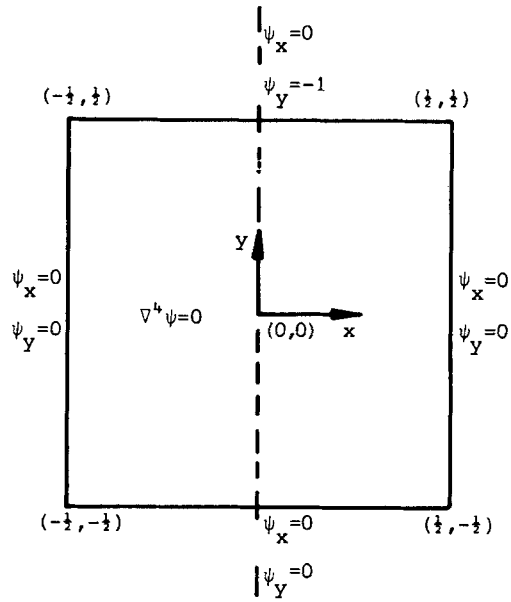

Figure 2. The driven cavity problem

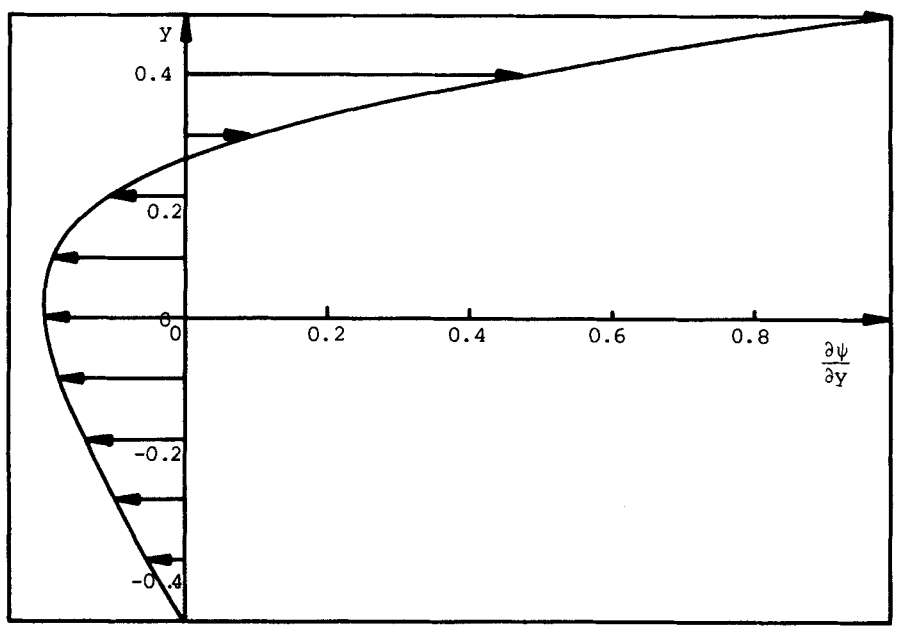

Figure 3. Velocity profile along the driven cavity centreline

Another quantity of interest is the vorticity $\nabla^2\psi$. In Figure 4 contour plots of approximations to the vorticity determined on a $\frac{1}{128}\times\frac{1}{64}$ grid with $M1=120$, $N1=12$, FEV1$=1500$, $M2=144$, $N2=14$ and FEV2$=4000$ are presented. These are virtually indistinguishable from the vorticity contours obtained by Kelmanson.[13]

In Figure 5 the final locations of the singularities near the boundary singularity are shown for the cases $M=200$, $N=16$, FEV$=2500$ and $M=160$, $N=13$, FEV$=3500$. These indicate that the MFS places several singularities in the vicinity of the boundary singularity, which is not surprising because the MFS representation is only valid if the auxiliary boundary formed by the singularities

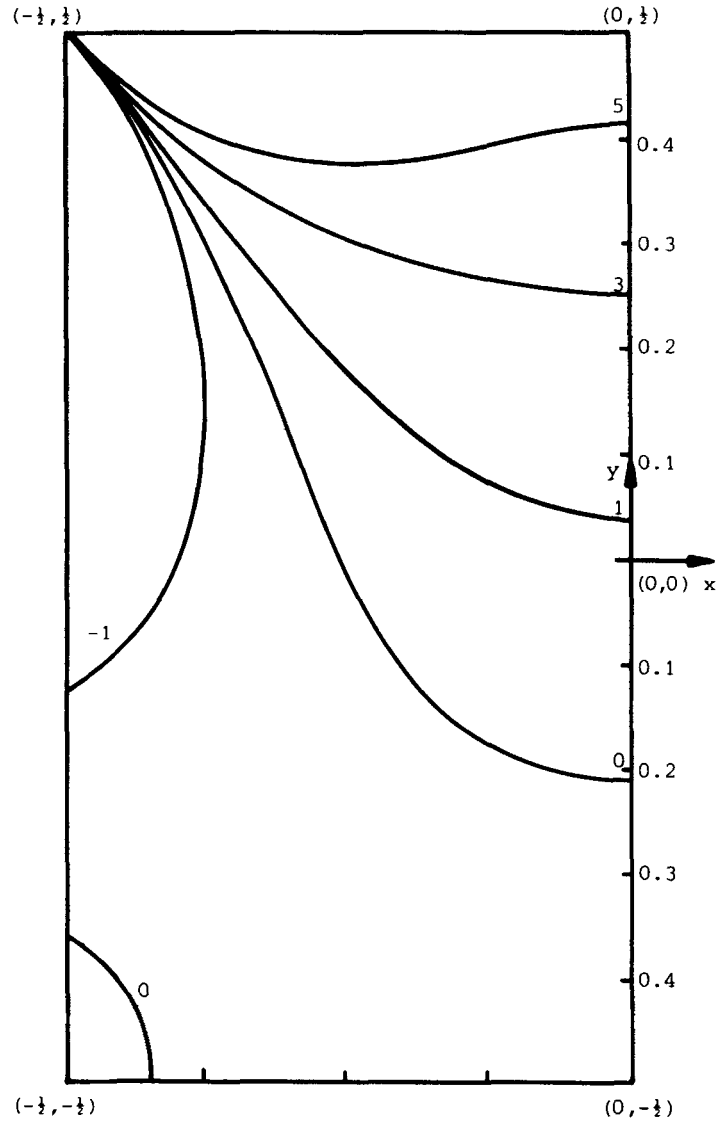

Figure 4. Vorticity contours for the driven cavity problem

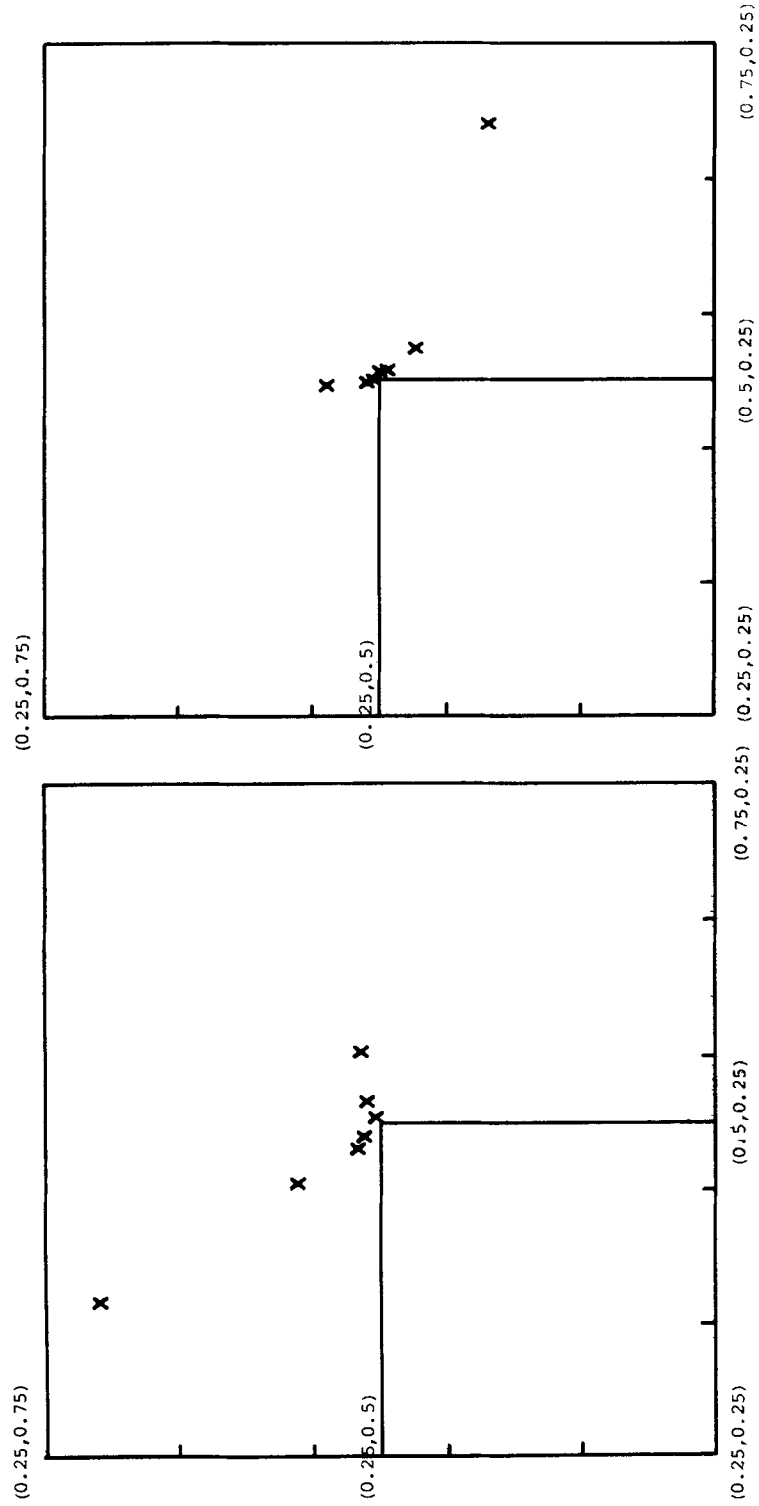

Figure 5. Observed typical behaviour of singularities

approaches the boundary of the region under consideration at the singular point. (See Fairweather and Johnston[3] and Oliveira.[8])

3.3 *Example 3—2:1 contraction flow*

The final problem examined in this study is planar Stokes flow through an abruptly changing channel with contraction ratio 2:1. This problem is considered by Black *et al.*[5] using a boundary integral equation formulation. The flow region and boundary conditions are shown in Figure 6.

Boundary points were placed on the boundary of the flow region in the following way. If $8M$ boundary points were used, M points were placed on each of the boundary segments AB, BC, CD, DE, EF, FG, GH and HA, and these were uniformly spaced along each segment. The reason for using a denser grid on each of the segments BC, CD, EF and FG is the presence of re-entrant corner singularities at the corners C and F.

In order to test the accuracy of the method, we examined the behaviour of the x-derivatives of the velocity $\partial\psi/\partial y$ along the centreline of the flow. Figures 7, 8 and 9 show the derivatives $(\partial/\partial x)(\partial\psi/\partial y)$, $(\partial^2/\partial x^2)(\partial\psi/\partial y)$ and $(\partial^3/\partial x^3)(\partial\psi/\partial y)$ respectively along the centreline $y=0$. The graphs of these quantities are plotted on the interval $-0{\cdot}2 \leq x \leq 0{\cdot}3$ and were obtained using the improved version of the MFS with $M1=200$, $N1=16$, $FEV1=2500$, $M2=248$, $N2=4$ and $FEV2=7500$. The results presented in Figures 7, 8 and 9 show good agreement with the corresponding results of Black *et al.*[5] The results for $(\partial/\partial x)(\partial\psi/\partial y)$, $(\partial^2/\partial x^2)(\partial\psi/\partial y)$ and $(\partial^3/\partial x^3)(\partial\psi/\partial y)$ on $0{\cdot}3 < x < 0{\cdot}5$ were poor because the finite location of the downstream boundary DE gives rise to errors in the x-derivatives of $\partial\psi/\partial y$ as $x \to 0{\cdot}5$, which propagate about 0·2 units into the flow field (see Black *et al.*)[5]

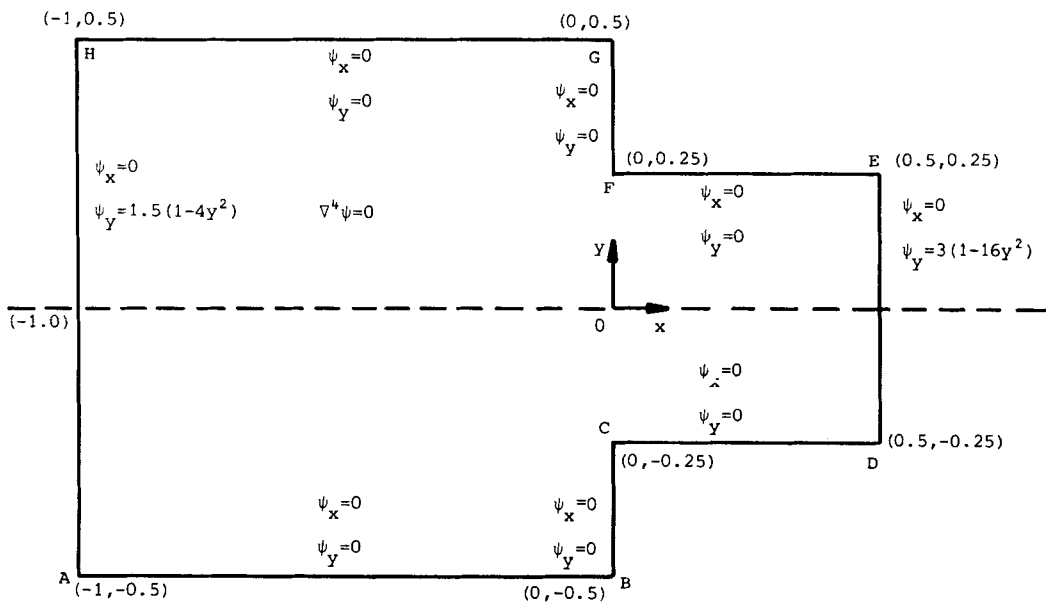

Figure 6. 2:1 contraction flow

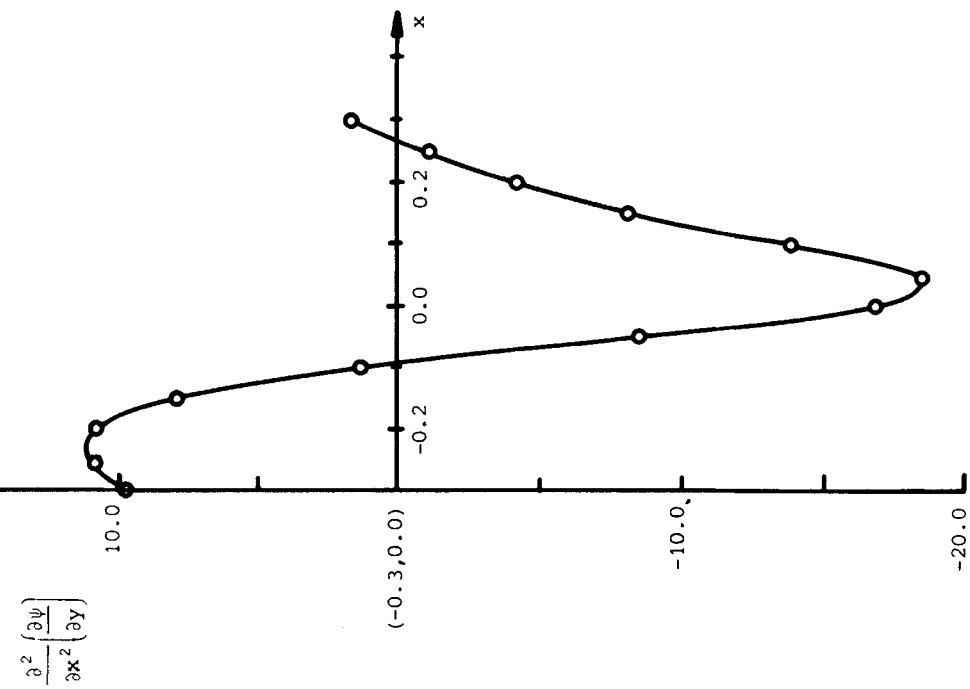

Figure 8. Centreline variation in $(\partial^2/\partial x^2)(\partial\psi/\partial y)$

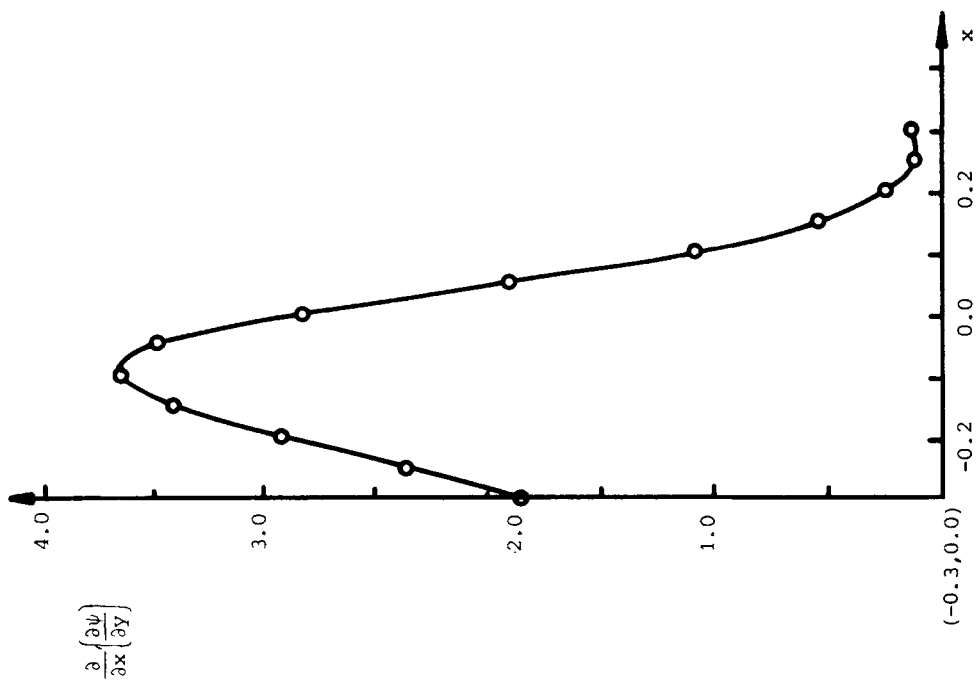

Figure 7. Centreline variation in $(\partial/\partial x)(\partial\psi/\partial y)$

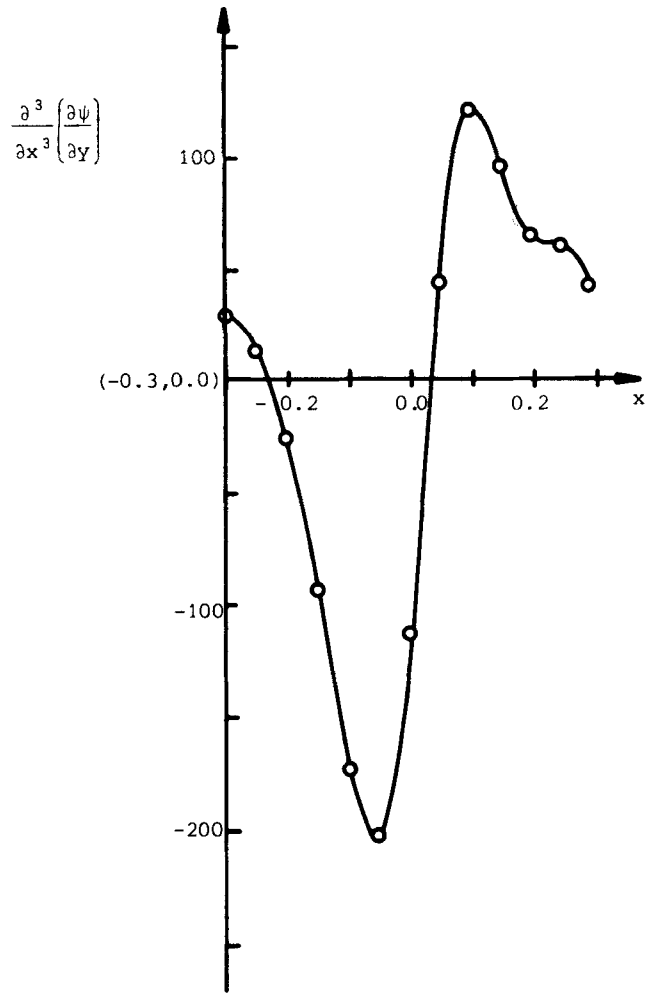

Figure 9. Centreline variation in $(\partial^3/\partial x^3)(\partial\psi/\partial y)$

4. CONCLUSIONS

In this study a new formulation of the method of fundamental solutions for solving biharmonic problems is presented. This formulation is based on the simple layer potential representation of Fichera and shares many of the features of the two previous formulations of the method of fundamental solutions for biharmonic problems.[1,2]

This formulation is ideally suited for solving problems in fluid flow where the velocities are prescribed on the boundary of the flow region. As was the case in the two previous formulations,[1,2] the present MFS, in contrast to the boundary integral formulation of the simple layer potential representation of Fichera (see Richter)[7] does not appear to be adversely affected by geometrical discontinuities.

The accuracy of the method is demonstrated by solving three problems arising in Stokes fluid flow. The results compare favourably with published results obtained using boundary integral

formulations. In comparison to the boundary element method, the MFS generally requires fewer degrees of freedom to produce results of a prescribed accuracy.

The main disadvantage of this formulation, as is the case for all MFS formulations, is the relatively large cost in computer time involved in applying the non-linear least squares minimization algorithm. This cost has been reduced by exploiting various degrees of symmetry which the problem might possess.

ACKNOWLEDGEMENTS

Portions of this work were performed while A. Karageorghis was a Visiting Researcher at the Center for Computational Sciences, University of Kentucky, Lexington, KY 40506, U.S.A. G. Fairweather was supported in part by funds from the National Science Foundation (Grant No. RII-8610671) and the Commonwealth of Kentucky through the Kentucky EPSCoR Program.

APPENDIX

If in expression (5) we replace, for simplicity, x_{p_i}, x_{t_j}, y_{p_j}, and y_{t_j} by x, x_j, y and y_j, respectively, and set

$$DX = x - x_j, \qquad DY = y - y_j, \qquad T1 = (DX)^2 + (DY)^2,$$

we may write

$$\psi_N = \sum_{j=1}^{N} \{c_j DX + d_j DY\} [\log(T1) + 1]. \tag{9}$$

From (1) and (2), we need to provide LMDIF with

$$f_i = \alpha(p) + \frac{\partial \psi_N}{\partial x}(p)$$

$$= \alpha(p) + \sum_{j=1}^{N} \left\{ c_j \left[\log(T1) + 1 + \frac{2(DX)^2}{T1} \right] + d_j \frac{2DX \cdot DY}{T1} \right\}, \quad i = 1, 2, \ldots, M, \tag{10}$$

$$f_i = \beta(p) + \frac{\partial \psi_N}{\partial y}(p)$$

$$= \beta(p) + \sum_{j=1}^{N} \left\{ c_j \frac{2DX \cdot DY}{T1} + d_j \left[\log(T1) + 1 + \frac{2(DX)^2}{T1} \right] \right\}, \quad i = M+1, M+2, \ldots, 2M. \tag{11}$$

Other quantities of interest are

$$\nabla^2 \psi_N, \quad \frac{\partial}{\partial x}\left(\frac{\partial \psi_N}{\partial y}\right), \quad \frac{\partial^2}{\partial x^2}\left(\frac{\partial \psi_N}{\partial y}\right), \quad \frac{\partial^3}{\partial x^3}\left(\frac{\partial \psi_N}{\partial y}\right),$$

and these are given by

$$\nabla^2 \psi_N = 4 \sum_{j=1}^{N} \left\{ c_j \frac{DX}{T1} + d_j \frac{DY}{T1} \right\}, \tag{12}$$

$$\frac{\partial}{\partial x}\left(\frac{\partial \psi_N}{\partial y}\right) = 2 \sum_{j=1}^{N} \left\{ c_j \left[\frac{-(DX)^2 \cdot DY + (DY)^3}{(T1)^2} \right] + d_j \left[\frac{(DX)^3 - DX \cdot (DY)^2}{(T1)^2} \right] \right\}, \tag{13}$$

$$\frac{\partial^2}{\partial x^2}\left(\frac{\partial \psi_N}{\partial y}\right)=\sum_{j=1}^{N}\left\{4c_j\left[\frac{(DX)^3\cdot DY-3DX\cdot(DY)^3}{(T1)^3}\right]+2d_j\left[\frac{-(DX)^4+6(DX)^2\cdot(DY)^2-(DY)^4}{(T1)^3}\right]\right\}, \tag{14}$$

$$\frac{\partial^3}{\partial x^3}\left(\frac{\partial \psi_N}{\partial y}\right)=\sum_{j=1}^{N}\left\{12c_j\left[\frac{-(DX)^4\cdot DY+6(DX)^2\cdot(DY)^3-(DY)^5}{(T1)^4}\right]\right.$$
$$\left.+4d_j\left[\frac{(DX)^5-14(DX)^3\cdot(DY)^2+9DX\cdot(DY)^4}{(T1)^4}\right]\right\} \tag{15}$$

respectively.

If, as in Examples 1 and 2, the problem has symmetry about the y-axis, then with $SX=x+x_j$ and $T2=(SX)^2+(DY)^2$, expressions (10)–(12) become

$$f_i=\alpha(p)+\sum_{j=1}^{N}\left\{c_j\left[\log\left(\frac{T1}{T2}\right)+\frac{2(DX)^2}{T1}-\frac{2(SX)^2}{T2}\right]+2d_jDY\left[\frac{DX}{T1}+\frac{SX}{T2}\right]\right\}, \quad i=1,2,\ldots,M, \tag{16}$$

$$f_i=\beta(p)+\sum_{j=1}^{N}\left\{2c_jDY\left[\frac{DX}{T1}-\frac{SX}{T2}\right]\right.$$
$$\left.+d_j\left[\log(T1\cdot T2)+2+\frac{2(DY)^2}{T1}+\frac{2(DY)^2}{T2}\right]\right\}, \quad i=M+1,M+2,\ldots,2M, \tag{17}$$

$$\nabla^2\psi_N=4\sum_{j=1}^{N}\left\{c_j\left[\frac{DX}{T1}-\frac{SX}{T2}\right]+d_jDY\left[\frac{1}{T1}+\frac{1}{T2}\right]\right\}. \tag{18}$$

REFERENCES

1. A. Karageorghis and G. Fairweather, 'The method of fundamental solutions for the numerical solution of the biharmonic equation', *J. Comput. Phys.*, **69**, 434–459 (1987).
2. A. Karageorghis and G. Fairweather, 'The Almansi method of fundamental solutions for solving biharmonic problems', *Int. j. numer. methods eng.*, **26**, 1665–1682 (1988).
3. G. Fairweather and R. L. Johnston, 'The method of fundamental solutions for problems in potential theory', in C. T. H. Baker and G. F. Miller (eds), *Treatment of Integral Equations by Numerical Methods*, Academic Press, London, 1982, pp. 349–359.
4. G. Fichera, 'Linear elliptic equations of higher order in two independent variables and singular integral equations with applications to anisotropic inhomogeneous elasticity', in *Partial Differential Equations and Continuum Mechanics*, University of Wisconsin Press, Madison, WI, 1961, pp. 55–80.
5. J. R. Black, M. M. Denn and G. C. Hsiao, 'Creeping flow of a viscoelastic liquid through a contraction: a numerical perturbation solution', in J. F. Hutton, J. R. A. Pearson and K. Walters (eds), *Theoretical Rheology*, Halsted Press, New York, 1975, pp. 3–30.
6. G. C. Hsiao and R. C. MacCamy, 'Solution of boundary value problems by integral equations of the first kind', *SIAM Rev.*, **15**, 687–705 (1973).
7. G. R. Richter, 'An integral equation method for the biharmonic equation', in R. Vichnevetsky (ed.), *Advances in Computer Methods for Partial Differential Equations—II*, IMACS(AICA), 1977, pp. 41–45.
8. E. R. Oliveira, 'Plane stress analysis by a general integral method', *J. Eng. Mech. Div. ASCE*, **94**, 79–101 (1968).
9. S. Ho-Tai, R. L. Johnston and R. Mathon, 'Software for solving boundary value problems for Laplace's equation using fundamental solutions', *Technical Report 136/79*, Department of Computer Science, University of Toronto, 1979.
10. M. MacDonell, 'A boundary method applied to the modified Helmholtz equation in three dimensions and its application to a waste disposal problem in the deep ocean', *M.S. Thesis*, Department of Computer Science, University of Toronto, 1985.
11. G. Burgess and E. Mahajerin, 'Rotational fluid flow using a least squares collocation technique', *Comput. Fluids*, **12**, 311–317 (1984).
12. M. S. Ingber and A. K. Mitra, 'Grid optimization for the boundary element method', *Int. j. numer. methods eng.*, **23**, 2121–2136 (1986).
13. M. A. Kelmanson, 'Modified integral equation solution of viscous flow near sharp corners', *Comput. Fluids*, **11**, 307–324 (1983).